SUPPORTING INFORMATION

Materials: Trioctylphosphine oxide (TOPO 99%) and Sulfur flakes (99.5%) were obtained from Aldrich. Trioctylphosphine (TOP, 97%), was purchased from Strem Chemicals. Octadecylphosphonic acid (ODPA, 99%) and hexylphosphonic acid (HPA, 99%) and Cadmium Oxide (CdO, 99.998%) were purchased from Alfa Aeser. MethoxyPEG-SH (5000 MW) was obtained from Rapp Polymere GmbH, Tuebingen, Germany. CdSe cores, used for nanorod growth, were synthesized following the previously published procedure.[1] PEGylated PIL-coated QDs were prepared as described earlier.[2]

Synthesis of CdSe/CdS nanorods: The nanorod synthesis procedure and control over nanorod length were obtained by modifying a previously published protocol.[1] In detail, TOPO (3g), ODPA (290mg), HPA (80mg) and CdO (87mg) were placed in a three neck 50mL flask. The mixture was degassed at 120°C for 20min (until the pressure dropped to 80 millitorr) and then the temperature was raised to 200°C under nitrogen atmosphere. At 200°C a thin needle (connected to a tube and condenser) was placed for 5min into a septum stopper to release water vapor formed by the cracking of CdO. After the pot solution turned colorless the temperature was raised to 300°C and 1.5mL of TOP was injected. The temperature was then raised to 350°C and a mixture of CdSe cores and TOP-S was injected. The amount of CdSe cores was a determining factor for the final length of the rods – it was varied from 80 to 10nmol to obtain rods of 17 to 72 nm in length, respectively. Freshly precipitated CdSe cores were mixed with 0.5mL of TOP in a glovebox and with 1.5mL of TOP-S (made by dissolving 1.2g of (S) in 15ml of TOP at 70°C). Following the injection of the cores and TOP-S the temperature of the pot was maintained at 350°C for 8min. After the nanorod solution cooled down, it was diluted with hexane to around 15mL of total volume. The concentration was calculated by approximating a 100% reaction yield with respect to the injected cores (i.e. nmol of obtained rods = nmol of injected cores).

Ligand exchange procedure: A portion of the rod growth solution (40µL, 0.96µM) was precipitated by addition of acetone (100µL) and centrifuged down (1500rcf). Next, 50µL of chloroform were added to the rod pellet. The nanorod solution was then added to a freshly prepared chloroform solution of MethoxyPEG$_{5K}$-SH (65mg in 100µL) placed in a septum-capped 3mL vial. Finally 20µL of 15nM $NaBH_4$ in methanol were added. The final mixture was stirred at 70°C under nitrogen atmosphere for 15min. At this point 100µL of 15nM $NaBH_4$ was added and the solution was stirred for a further 5min at 70°C under nitrogen atmosphere. The final solution was diluted with 200µL of ethanol and the nanorods were precipitated by adding hexanes. After 2min of centrifugation at 1800rcf, the supernatant was discarded and the nanorods were dissolved in 200µL of methanol. The methanol was pulled off

in vacuum and 1x PBS was then added to the nanorods. The rod solution was filtered through a 200nm syringe filter, dialyzed in a centrifugation filter (50,000 MW cut off, cellulose, Millipore), filtered once more through a 100nm centrifugation filter and stored at 4°C.

Synthesis of inverse-micelle encapsulated QDs in silica: The procedure was adopted from the literature.[3] In detail, anhydrous cyclohexane (70 mL) was added to 4.33 mL of Igepal CO-520 placed in a 500 mL round bottom flask, followed by vigorous stirring for 15 min. CdSe/CdS QDs capped with oleylamine and eleic acid[2] (3.3 nmol) were precipitated by the addition of 1 mL of acetone and centrifuged at 4000 RPM for 3 min. The supernatant was discarded while the pellet was dissolved in 1 mL of cyclohexane and then added to the stirred Igepal solution. After 15 min of stirring, TEOS was added (267 µL). Finally, after 30 min of stirring, 500 µL of ammonium hydroxide (28% in water) was slowly added and the mixture was stirred under nitrogen for 48 h at RT. The reaction solution was mixed with 50 mL of ethanol and centrifuged at 10000 RPM for 30 min. The supernatant was discarded and the process was repeated 2 more times with pure ethanol. Then, 5 mL of water containing 20 µL of 2M NaOH were added. The solution was sonicated for 1 min and centrifuged at 2500 RPM for 3 min in order to remove any aggregates. Supernatant containing QDs encapsulated with silica shells was stored at 4 C.

PEG coating: The particles (300 l) were mixed with 10 mL water containing 50 µL of ammonium hydroxide (28% in water) and sonicated for 5 min. To this solution 15 µL of TEOS were added, followed by 50 mg of methoxyPEG5000-silane (Laysan Bio Inc) in 1 mL of water. The vigorously stirred reaction mixture was kept at 70 C for 3.5 h and at RT for an additional 12 h, after which it was dialyzed through a 100K Millipore regenerated cellulose centrifugation filter three times, and finally dispersed in 1 mL of water. The obtained particles were stored at 4 C.

Nanoparticle characterization: Transmission electron microscopy (TEM) and ζ-potential measurements were carried out as described previously.[4] Dynamic light scattering (DLS) measurements were performed on a DynaPro Titan Dynamic Light Scatterer (Wyatt Technology Corporation).

Serum protein adsorption: Protein adsorption was measured after incubating the particle solution (50µL, 0.5mg solid content) with 50µL of Fetal Bovine Serum in a 1:1 ratio for 2hrs at 37°C. Samples incubated in PBS were used as controls. After incubation, the samples were diluted in PBS and their diffusion times were measured by fluorescence correlation spectroscopy (FCS) using a setup described previously.[5] Samples were excited at 1.8µW (power in front of the microscope objective), and seven to nine measurements with acquisition times of 60s each

were performed for each sample. Correlation functions were fit in Matlab (The Mathworks) with the isotropic 2D translational diffusion model to extract the average particle diffusion time. The diffusion times of nanorod and nanosphere samples incubated with FBS and PBS were compared.

Transmembrane diffusion: Membrane diffusion experiments were performed in a custom-built two-chamber setup. The chambers (source and recipient, 0.38mL in volume each) were connected through a thin membrane (Isopore membrane filter, Milipore) with different pore sizes (5µm, 400nm, 200nm, and 100nm). The effective area of the membranes exposed to the solutions was 11mm in diameter. The membranes were wetted prior the experiments by running a PBS solution through them. The source chamber was filled with a nanoparticle solution in PBS (~0.1µM) while the recipient chamber was filled with a pure PBS solution. Aliquots were taken simultaneously from both chambers in intervals of 15min (total time 135min) and the absorption was measured using a plate reader, after which the aliquots were returned to the chambers. Concentrations were directly calculated using the extinction coefficients at 350nm for QD-spheres and rods. All diffusion experiments were performed in 3 repetitions. Permeability values were calculated using $P = \frac{d}{dt}\left(-\ln[\frac{(2C(t)-C_0)V}{2C_0A}]\right)$, where P is the permeability, C(t) is the concentration in the source chamber at time t, C_0 is the initial source chamber concentration, V is chamber volume, and A is the membrane area.

Collagen gel diffusion: A detailed description of collagen gel diffusion experiments can be found elsewhere.[5]

Tumor models: Orthotopic mammary tumor models were prepared by implanting a small piece (1mm^3) of viable tumor tissue from a source tumor animal into severe combined immunodeficient (SCID) mice bearing mammary fat pad chambers.[6] The tumors were allowed to grow to 5mm in diameter. All animal procedures were carried out following the Public Health Service Policy on Humane Care of Laboratory Animals and approved by the Institutional Animal Care and Use Committee of Massachusetts General Hospital.

In vivo imaging: A mixture of the two nanoparticles was prepared for intravenous injection. Concentrations were adjusted with in vitro calibration to result in roughly equal photoluminescence intensity for all three nanoparticle samples under 800nm multiphoton excitation. Following retro-orbital injection of 200µL with these concentrations, multiphoton imaging was carried out as described previously[7] on a custom-built multiphoton laser-scanning microscope using confocal laser-scanning microscope body (Olympus 300; Optical Analysis Corp.) and a broadband femtosecond laser source (High Performance MaiTai, Spectra-Physics). Image slices were taken at ~60mW at sample surface with depths from 0 - 201µm, with 2.76µm steps and 2.76x2.76µm pixels. Mosaic images

were taken in raster pattern using a motorized stage (H101, Prior Scientific, Inc.) and customized automation software (LabView, National Instruments). Imaging studies were performed with a 20X magnification, 0.95NA water immersion objective (Olympus XLUMPlanFl, 1-UB965, Optical Analysis).

Image analysis: Images were analyzed using custom analysis software developed in Matlab (The Mathworks). The analysis approach involved 3D vessel tracing[8] to create vessel metrics and a 3D map of voxel intensity versus distance to the nearest vessel over time. Images were also corrected for sample movement over time with 3D image registration. The normalized transvascular flux was calculated using $\frac{J_t}{S_v(C_v-C)} = P_{eff} = \lim_{t\to 0} \frac{\partial}{\partial t} \frac{\int_{r=R}^{\infty} C(r) r \partial r}{(C_v-C)R}$, where J_t is the transvascular flux, S_v is the vessel surface area, C_v is the concentration of the probe in the vessel, C is the concentration of the probe immediately extravascular, P_{eff} is the effective permeability,[7] t is time after the initial image, r is the distance from the vessel central axis, and R is the vessel radius at that point along the vessel. Fluorescence intensities were used as equivalent to these concentrations for the calculations. Each calculation was made as an average over the entire imaged volume for each tumor. Nanoparticle distribution was calculated by first subtracting the intensity of each voxel in the imaged tumor volume shortly following injection from the intensity of each corresponding voxel 1hr after injection. After this background subtraction, the fraction of voxels greater than zero was taken as the volume fraction of each tumor containing nanoparticles.

Blood clearance half-lives: Blood clearance half-lives measurements were performed as described previously.[2]

SUPPORTING TABLES

Supporting Table 1. Thickness of the nanoparticle PEG layer. We measured the inorganic and effective hydrodynamic sizes of two sets of QDs capped with a PEG_{5k} ligand using TEM and DLS respectively. We then calculated the size difference to estimate the thickness of the PEG layer.

QD sample	Inorganic diameter (TEM) / nm	Hydrodynamic diameter in PBS (DLS) / nm	Diameter size difference (DLS – TEM) / nm
QD_1-PEG_{5K}	7.2 ± 0.5	17.6 ± 0.9	10.4 ± 1.0
QD_2-PEG_{5K}	4.0 ± 0.3	15.0 ± 0.2	11.0 ± 0.4

Supporting Table 2. Nanoparticle size. We measured the inorganic and effective hydrodynamic sizes of the nanoparticles (nanospheres, nanorods, and PEGylated PIL-QDs) with TEM and DLS, respectively.

	inorganic size (TEM) / nm	Hydrodynamic size (DLS) / nm	Hydrodynamic aspect ratio	Diffusion constant / $\times 10^{-7} cm^2 s^{-1}$
nanosphere	30.3 ± 2.4	34.8 ± 1.6	1	1.39 ± 0.06
nanorod	44.0 ± 3.5 (long) 4.7 ± 0.5 (thick)	32.9 ± 1.3	~3.6*	1.46 ± 0.05
QD	7.2 ± 0.5	12.8 ± 0.3	1	3.76 ± 0.08

*considering 5nm PEG layer.

SUPPORTING FIGURES

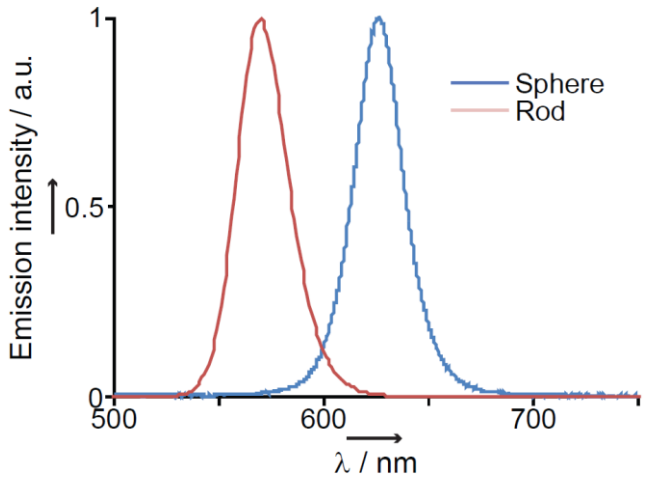

Supporting Figure 1. Emission spectra for the nanospheres and nanorods. We collected images using a 585nm dichroic mirror separating into 560±20nm (nanorod channel) and 635±20nm (nanosphere channel) bandpass filters.

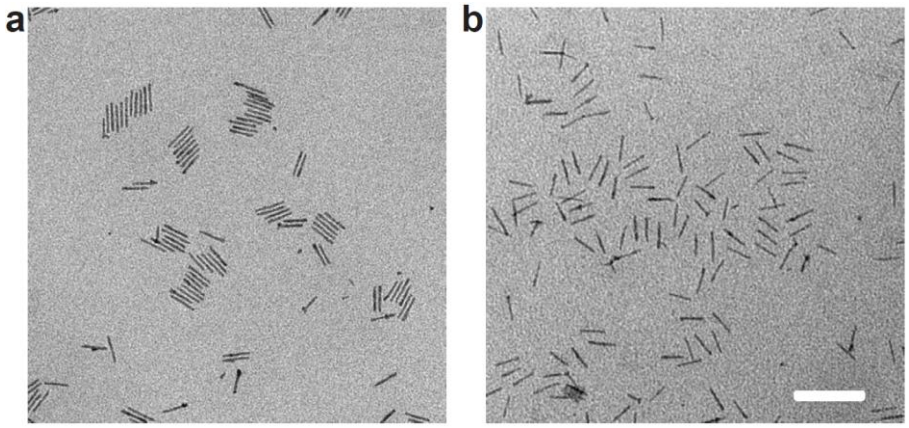

Supporting Figure 2. Thickness of the nanoparticle PEG layer. We collected TEM images of nanorods capped (**a**) with trioctylphosphine (TOPO) ligands and (**b**) with PEG_{5K} ligands. Scale bar - 100nm. The average inter-rod distances were (**a**) 2.7 ± 0.3nm and (**b**) 12.1 ± 1.3nm.

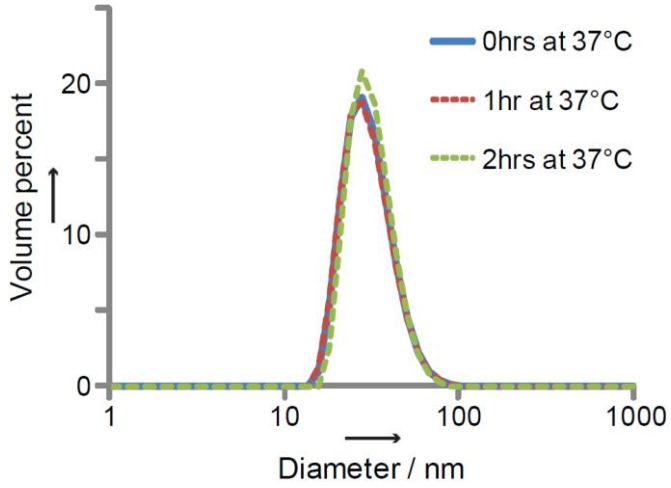

Supporting Figure 3. Nanorod stability over time. We measured dynamic light scattering (DLS) data for the nanorods at RT in PBS (blue line), after 1h at 37°C (red dotted line), and after 2h at 37°C (green dotted line). Nanorod size was stable over this incubation time.

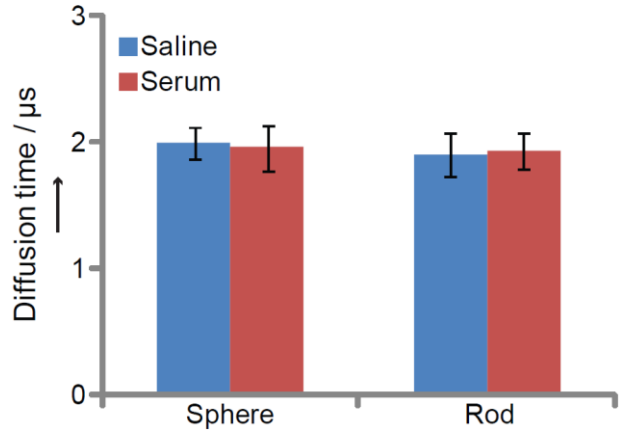

Supporting Figure 4. Protein adsorption on the nanospheres and nanorods following incubation in serum. We measured diffusion times for the nanospheres and nanorods by fluorescence correlation spectroscopy after incubation at 37°C in fetal bovine serum (FBS) and in PBS. The diffusion times of the nanospheres and nanorods in both PBS and FBS were within experimental error, indicating that protein adsorption was negligible.

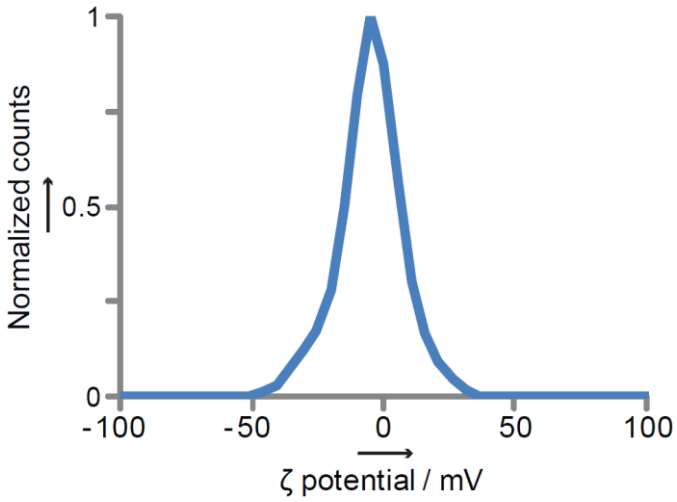

Supporting Figure 5. Nanorod surface charge. We measured the ζ potential of nanorods capped with PEG_{5K} ligand. We found that the mean ζ potential was -4.9 ± 6.2mV.

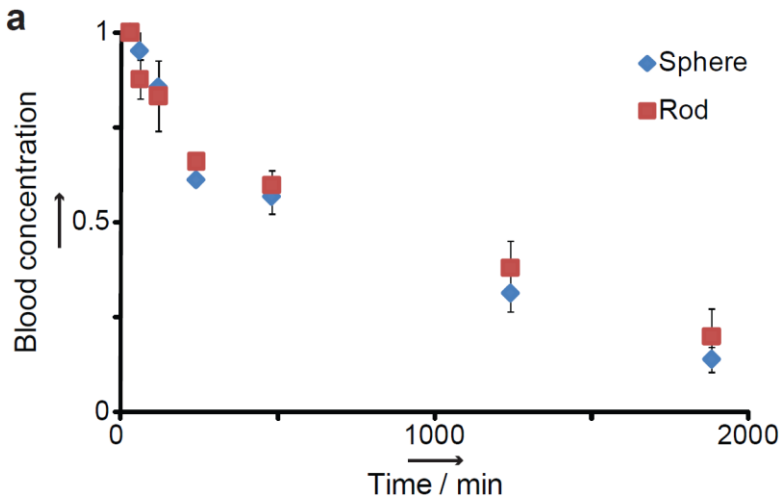

b

Particle	Clearance half-life / min
Sphere	736 +/- 81
Rod	933 +/- 160

Supporting Figure 6. Nanoparticle clearance from the blood for nanospheres versus nanorods of the same hydrodynamic diameter (~33-35nm). (a) Nanoparticle blood concentration in tumor-free female SCID mice. (b) The β plasma half-life – representing clearance from the blood following uptake by the organs – for both nanoparticles. The data suggest that the two particles are taken up by normal organs and clear from the body at roughly the same rates.

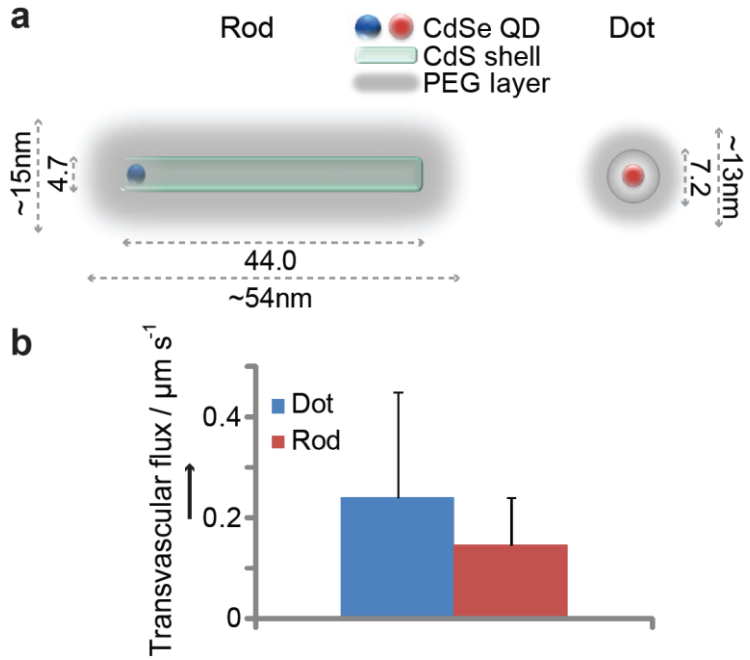

Supporting Figure 7. Transvascular transport rates for nanorods (14.7nm diameter, 54nm length) versus PEGylated PIL-coated quantum dots of roughly the same diameter (12.8nm). (**a**) A schematic of the nanoparticles used. (**b**) Nanorod versus quantum dot transvascular transport. We measured these transport rates in orthotopic E0771 mammary tumors in mice, quantified as nanoparticle transvascular mass flux per the vascular surface area and transvascular concentration difference, also called the effective permeability. The nanorods transport across vessel walls about as rapidly as the quantum dots, suggesting the importance of the small dimension for transport through pores.

SUPPORTING REFERENCES

[1] L. Carbone, C. Nobile, M. De Giorgi, F. D. Sala, G. Morello, P. Pompa, M. Hytch, E. Snoeck, A. Fiore, I. R. Franchini, M. Nadasan, A. F. Silvestre, L. Chiodo, S. Kudera, R. Cingolani, R. Krahne, L. Manna, *Nano Lett.* **2007**, *7*, 2942.

[2] R. Koole, M. M. van Schooneveld, J. Hilhorst, C. D. Donega, D. C. `t Hart, A. van Blaaderen, D. Vanmaekelbergh, A. Meijerink, *Chem. Mater.* **2008**, *20*, 2503.

[3] W. Liu, A. B. Greytak, J. Lee, C. R. Wong, J. Park, L. F. Marshall, W. Jiang, P. N. Curtin, A. Y. Ting, D. G. Nocera, D. Fukumura, R. K. Jain, M. G. Bawendi, *J. Am. Chem. Soc.* **2010**, *132*, 472.

[4] Z. Popović, W. Liu, V. P. Chauhan, J. Lee, C. Wong, A. B. Greytak, N. Insin, D. G. Nocera, D. Fukumura, Jain, M. G. Bawendi, *Angew. Chem. Int. Ed.* **2010**, *49*, *8649*.

[5] C. Wong, T. Stylianopoulos, J. Cui, J. Martin, V. P. Chauhan, W. Jiang, Z. Popovic, R. K. Jain, M. G. Bawendi, D. Fukumura, *Proc. Natl. Acad. Sci. U. S. A.* **2011**, *108*, 2426.

[6] B. J. Vakoc, R. M. Lanning, J. A. Tyrrell, T. P. Padera, L. A. Bartlett, T. Stylianopoulos, L. L. Munn, G. J. Tearney, D. Fukumura, R. K. Jain, B. E. Bouma, *Nat. Med.* **2009**, *15*, 1219.

[7] E. B. Brown, R. B. Campbell, Y. Tsuzuki, L. Xu, P. Carmeliet, D. Fukumura, R. K. Jain, *Nat. Med.* **2001**, *7*, 864.

[8] J. A. Tyrrell, V. Mahadevan, R. T. Tong, E. B. Brown, R. K. Jain, B. Roysam, *Microvasc. Res.* **2005**, *70*, 165.